

Short communication

Adipic acid assisted, sol–gel route for synthesis of $\text{LiCr}_x\text{Mn}_{2-x}\text{O}_4$ cathode material

R. Thirunakaran^{a,*}, Ki-Tae Kim^b, Yong-Mook Kang^b,
Chan-Yeo Seo^b, Jai Young-Lee^b

^a Central Electrochemical Research Institute, Electrochemical Power Systems Division, Karaikudi 630 006, India

^b Department of Material Science and Engineering, Korea Advanced Institute of Science and Technology, 373-1, Gusong-Dong, Yusong-Gu, Daejeon, Republic of Korea

Received 25 November 2003; accepted 11 February 2004

Available online 11 August 2004

Abstract

Spinel LiMn_2O_4 and $\text{LiCr}_x\text{Mn}_{2-x}\text{O}_4$ ($x = 0.00–0.20$) have been synthesized by a soft chemistry method using adipic acid as the chelating agent. This technique offers better homogeneity, preferred surface morphology, reduced heat-treatment conditions, sub-micron sized particles, and better crystallinity. The synthesized spinel materials are characterized by X-ray diffraction, scanning electron microscopy, cyclic voltammetry, and charge–discharge testing. It is found that chromium substitution alleviates capacity fading in the 4-V region and improves the structural stability of LiMn_2O_4 spinel upon repeated cycling.

© 2004 Published by Elsevier B.V.

Keywords: Spinel LiMn_2O_4 ; Chromium substitution; Adipic acid; Sol–gel synthesis; Intercalation reaction; Electrochemical properties; Lithium ion battery

1. Introduction

LiMn_2O_4 spinel is a promising cathode material for rechargeable lithium batteries because of its low cost and environmentally benign nature. Although LiMn_2O_4 cycles well at room temperature, prolonged cycling at higher temperatures is accompanied by an unacceptable fading of capacity [1,2]. This phenomenon has been attributed to several factors such as electrolyte decomposition, slow dissolution of LiMn_2O_4 [3], unstable two-phase reaction, i.e., Jahn-Teller distortion [4], lattice instability [5], and particle disruption [6]. Ohzuku et al. [7] have studied a series of 5-V positive-electrode (cathode) materials obtained by substituting the Mn in LiMn_2O_4 with third transition metals such as Co, Cr, Cu, Fe, Ni, Ti and Zn, which are effective in suppressing capacity fading on cycling. These materials have operating voltages above 4.8 V, as also reported by Lee et al. [8].

It is well known that the physical as well as the electrochemical properties of any cathode depend upon the method of synthesis and the type of precursors employed. In recent years, several low-temperature preparation methods, such as

sol–gel synthesis [9,10], precipitation [11], the Pechini process [12], and a hydrothermal method [13] have been used to prepare LiMn_2O_4 . In this work, an attempt has been made to stabilize the LiMn_2O_4 spinel structure by a sol–gel method that employs adipic acid as a chelating agent with Cr as a dopant. This soft chemistry technique offers many advantages such as better homogeneity, low calcination temperature, shorter heating time, regular morphology, sub-micron sized particles, less impurities, large surface area, and good control of stoichiometry.

2. Experimental

$\text{LiCr}_x\text{Mn}_{2-x}\text{O}_4$ ($x = 0.00, 0.01, 0.02, 0.05, 0.10, 0.20$) powders have been synthesized by a sol–gel method using adipic acid as a chelating agent, see Fig. 1. Stoichiometric amounts of lithium nitrate, manganese nitrate, and ammonium dichromate were mixed thoroughly and dissolved in de-ionized water. The solution was stirred continuously with mild heating to ensure homogeneity. The 50 ml of 1 M adipic acid was added to the homogeneous solution and resulted in the formation of precipitate. Simultaneously, the pH of the solution was adjusted to between 7 and 8.5 and stirring and heating was continued until a gel was obtained.

* Corresponding author. Tel.: +91-4565-22322; fax: +91-4565-37779.
E-mail address: rthirunakaran@yahoo.com (R. Thirunakaran).

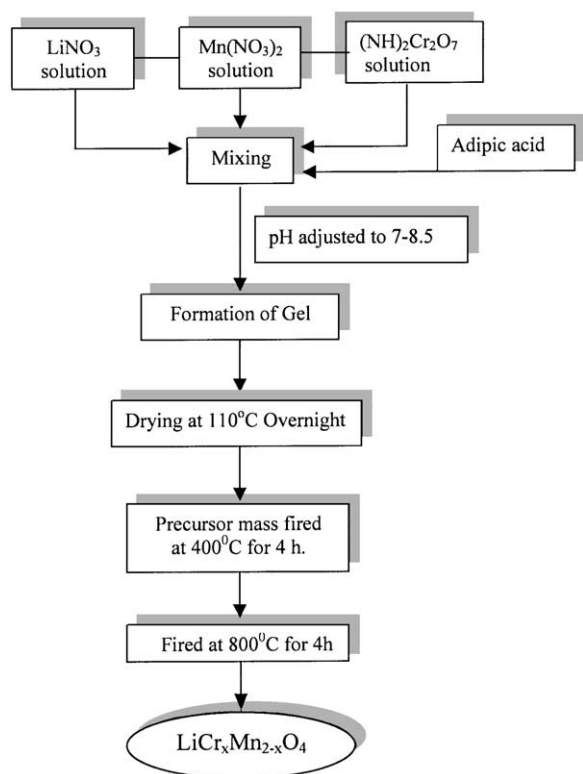


Fig. 1. Flow chart for synthesis of $\text{LiCr}_x\text{Mn}_{2-x}\text{O}_4$ via adipic assisted, sol-gel route.

The gel thus obtained was heated initially in an oven at 110°C overnight and then in a furnace at 400°C for about 4 h. Finally, the powder was heated at 800°C for 4 h to ensure good purity and crystallinity. Ultimately, the resulting

powders were subjected to physical as well as electrochemical characterization.

2.1. Coin cell preparation

Standard 2016 coin cells were assembled using lithium metal as the anode, a Celgard 2400 separator, and a 1 M solution of LiPF_6 in a 50:50 (v/v) mixture of ethylene carbonate and dimethyl carbonate as electrolyte. The cathode was an aluminium disc (diameter 1.8 cm) that was spread-coated with a 80:10:10 slurry of the cathode active powder, graphite and polyvinylidene fluoride in *N*-methyl-2-pyrrolidone. The loading of active material in the cathode varied from 0.087 to 0.098 g. Charge–discharge studies were carried out between 3 and 4.5 V by wears of an in-house charging facility.

Phase characterization studies were undertaken on a Jeol JDX 8030 X-ray diffractometer with nickel-filtered $\text{Cu K}\alpha$ radiation, in order to examine the crystalline phase of the synthesized spinel. The surface morphology was investigated with a JEOL JSM 1200 EX II scanning electron microscope (SEM). Charge–discharge studies were performed with a TOSCAT-3000 V, battery testing unit. The cells were assembled in an argon-filled glove-box (MBraun) with moisture and oxygen levels maintained at less than 1 ppm.

3. Results and discussion

3.1. X-ray diffraction analysis

The X-ray diffraction patterns of Cr^{3+} -doped samples show striking similarity to that of pure LiMn_2O_4 (space

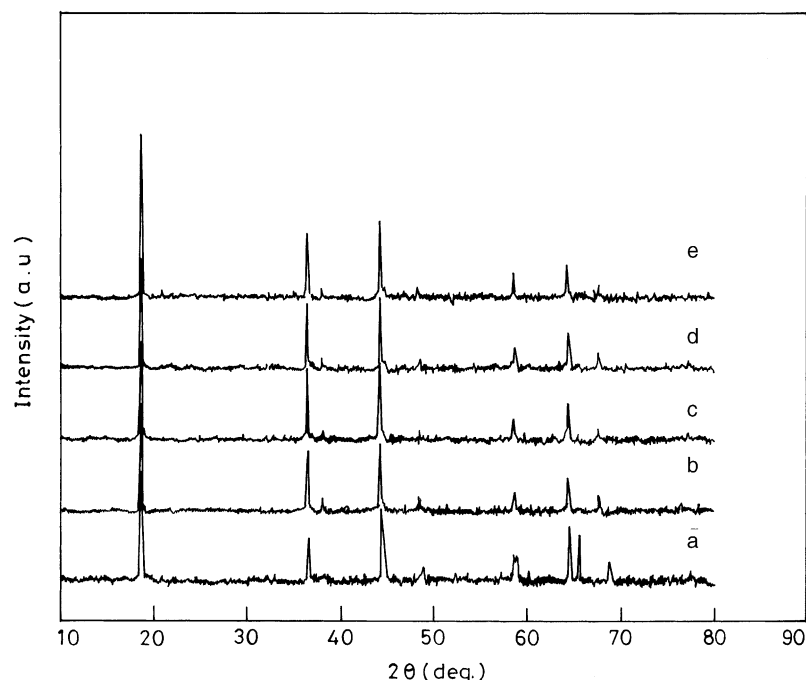
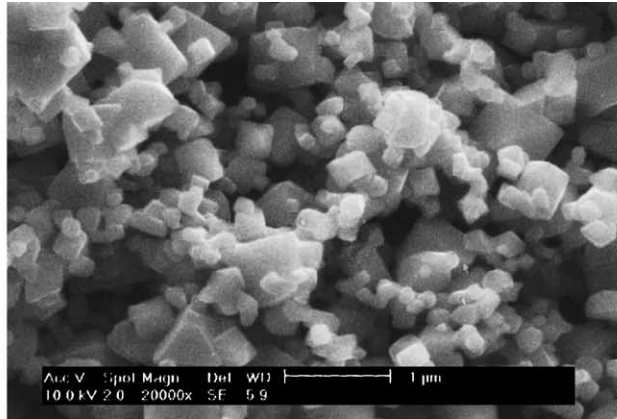


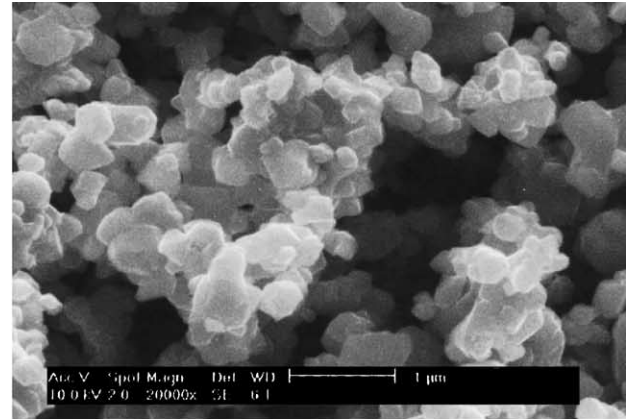
Fig. 2. XRD pattern for $\text{LiCr}_x\text{Mn}_{2-x}\text{O}_4$ samples calcined at 800°C for 4h: (a) $x = 0.00$, (b) $x = 0.01$, (c) $x = 0.02$, (d) $x = 0.05$, (e) $x = 0.10$.

group Fd3m) in which the manganese ions occupy the 16d sites and the O²⁻ ions occupy the 32c sites (Fig. 2). That the chromium-doped compounds have cubic spinel structure has been demonstrated by several workers [14–16]. In fact, the lattice parameters of LiCr_xMn_{2-x}O₄ are very close to those of LiMn₂O₄ [17–19]. Substitution of manganese by chromium should result in a shrinkage of the unit-cell volume. This is because, in the same oxidation state, chromium

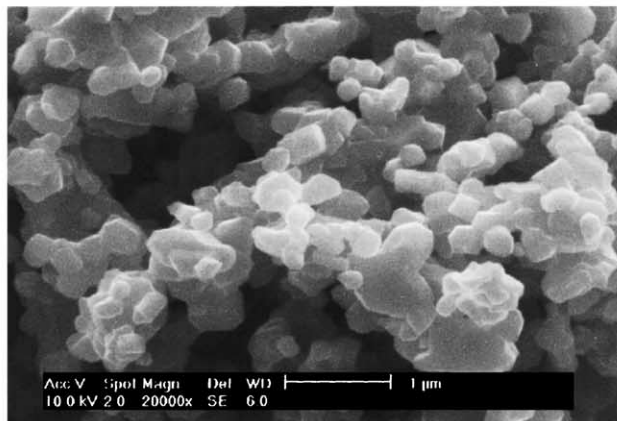
ions have smaller ionic radii than manganese ions, i.e., Cr³⁺ (0.615 Å), Mn³⁺ (0.68 Å), Cr⁴⁺ (0.58 Å), Mn⁴⁺ (0.60 Å) [20]. The decrease in cell volume should increase the stability of the structure during intercalation and de-intercalation of lithium [21–23]. The stronger Cr–O bonds in the delithiated state (compare the binding energy of 1142 kJ mol⁻¹ for CrO₂ with 946 kJ mol⁻¹ for α-MnO₂) may also be expected to contribute to stabilization of the octahedral sites.



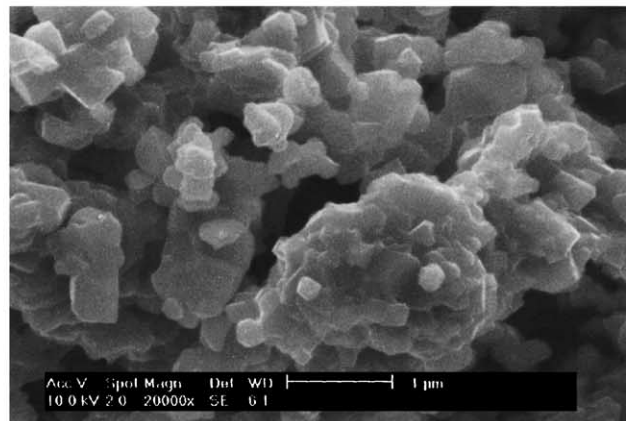
Undoped LiMn₂O₄ 800 °C



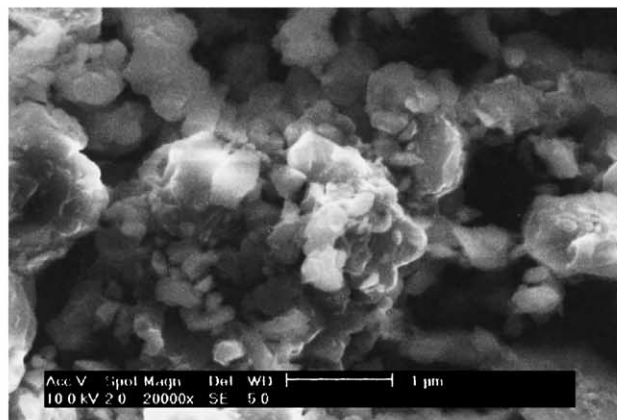
0.01 Cr doped – LiMn₂O₄ 800 °C



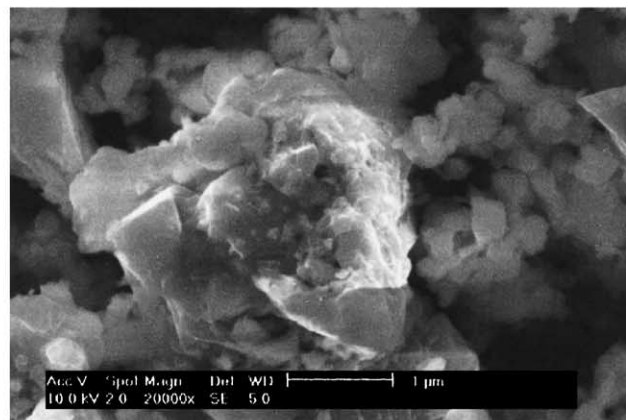
(a) 0.02 Cr doped – LiMn₂O₄ 800 °C



0.05 Cr doped – LiMn₂O₄ 800 °C



(b) 0.1 Cr doped – LiMn₂O₄ 800 °C



0.2 Cr doped – LiMn₂O₄ 800 °C

Fig. 3. Scanning electron micrographs for sample calcined at 800 °C for 4h: (a) $x = 0.00$, (b) $x = 0.01$, (c) $x = 0.02$, (d) $x = 0.05$, (e) $x = 0.10$, (f) $x = 0.20$.

The higher stabilization energy of Cr^{3+} ions for octahedral coordination is well known. Sigala et al. [21] have demonstrated the structural stability imparted by Cr^{3+} ions to LiMn_2O_4 spinels, and a similar effect by chemically modified Cr^{5+} – Cr^{6+} oxide has been observed by Zhang et al. [22]. It has also been found [23] that incorporation of Cr^{3+} greatly suppresses the dissolution of manganese ions in the electrolyte, which is one of the failure of mechanisms of LiMn_2O_4 cathodes.

3.2. Surface morphology

Surface morphology, one of the prime factors that govern the physical as well as the electrochemical properties of synthesized cathode oxides, has been studied by means of SEM analysis. The micrographs for a series of $\text{LiCr}_x\text{Mn}_{2-x}\text{O}_4$ ($x = 0.00, 0.01, 0.02, 0.05, 0.10, 0.20$) samples are given in Fig. 3. It is evident that the presence spherical grains of an independent nature are obtained up to a dopant level of about $x = 0.02$. Slightly agglomerated particles are formed at higher dopant concentrations of $x = 0.05, 0.10, 0.20$.

It is interesting to note that the effect of a high calcination temperature results in the formation of highly sintered particles, as demonstrated by the micrographs. Nevertheless, particles of sub-micron size ($<0.10\ \mu\text{m}$) are present throughout the series of solid solutions of $\text{LiCr}_x\text{Mn}_{2-x}\text{O}_4$ ($x = 0.00$ – 0.20). The sintered nature of particles of uniformly distributed, sub-micron size is desirable for cathode materials as they enhance the electrochemical behaviour. Evidently, the present sol–gel approach, in which adipic acid is used as a chelating agent, has resulted in the formation of particles that possess preferred surface morphology.

3.3. Charge–discharge studies

Charge–discharge curves for LiMn_2O_4 and $\text{LiCr}_x\text{Mn}_{2-x}\text{O}_4$ cells are given in Fig. 4. These cells were cycled between 3 and 4.25 V at the $0.1\ ^\circ\text{C}$ rate. The two-step

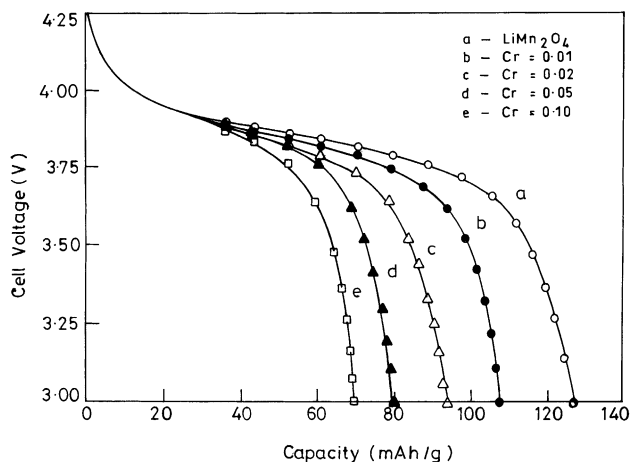
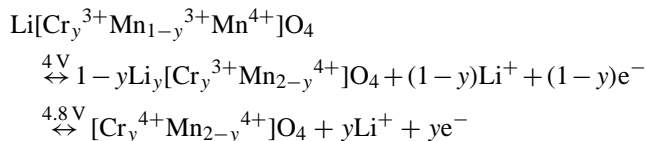


Fig. 4. Charge–discharge behaviour of LiMn_2O_4 and $\text{LiCr}_x\text{Mn}_{2-x}\text{O}_4$ cells: (a) $x = 0.00$, (b) $x = 0.01$, (c) $x = 0.02$, (d) $x = 0.05$, (e) $x = 0.10$.

intercalation–de-intercalation process for chromium-doped LiMn_2O_4 can be represented as follows:



During the first cycle, the LiMn_2O_4 spinel exhibits a specific capacity of $128\ \text{mA h g}^{-1}$, whereas 0.01 Cr-doped material gives a slightly lower capacity. Replacement of Mn^{3+} ion by Cr^{3+} and the oxidation of a similar amount of Mn^{3+} to the Mn^{4+} state leads to an increase in the average oxidation state of manganese. The diminished Mn^{3+} ion concentration causes a reduction in the unit-cell volume of the spinel, which results in increased structural stability. The capacities obtained correspond to oxidation of Mn^{3+} to Mn^{4+} . The oxidation of Cr^{3+} to Cr^{4+} occurs at 4.8 V [24–27].

3.4. Cycleability studies

The cycleability curves for pure LiMn_2O_4 and chromium-doped spinel are shown in Fig. 5. It is seen that 0.01 chromium-doped LiMn_2O_4 exhibits a constant capacity up to 100 cycles. The superior cycleability of the doped variety is due to increased stability caused by the higher octahedral site stabilization energy of Cr^{3+} . The effect of chromium is more pronounced in reducing the capacity fade. On the other hand, the cycleability of undoped LiMn_2O_4 decreases drastically. Undoped LiMn_2O_4 delivers an initial capacity of $120\ \text{mA h g}^{-1}$, whereas 0.01Cr gives a constant capacity of $110\ \text{mA h g}^{-1}$.

3.5. Cyclic voltammetric studies

Cyclic voltammograms (sweep rate: $0.02\ \text{mV s}^{-1}$) for cells with LiMn_2O_4 and $\text{LiCr}_{0.01}\text{Mn}_{1.99}\text{O}_4$ are presented in Fig. 6a and b, respectively. Despite electrolyte decomposition is a possibility at the high voltage that is used there is no evidence for this in the voltammograms. Indeed, LiPF_6 -based electrolytes, such as that used were

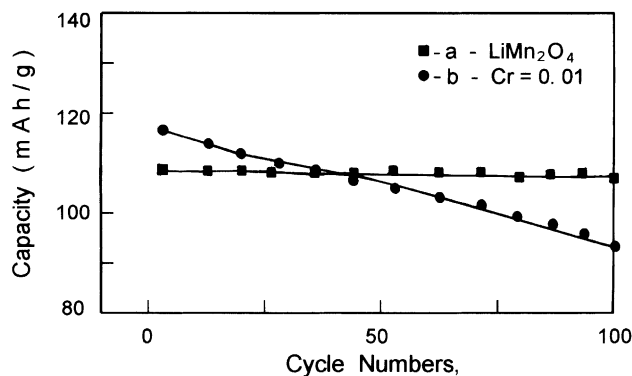


Fig. 5. Cycling performance of (a) LiMn_2O_4 and (b) $\text{LiCr}_{0.01}\text{Mn}_{1.99}\text{O}_4$ cells.

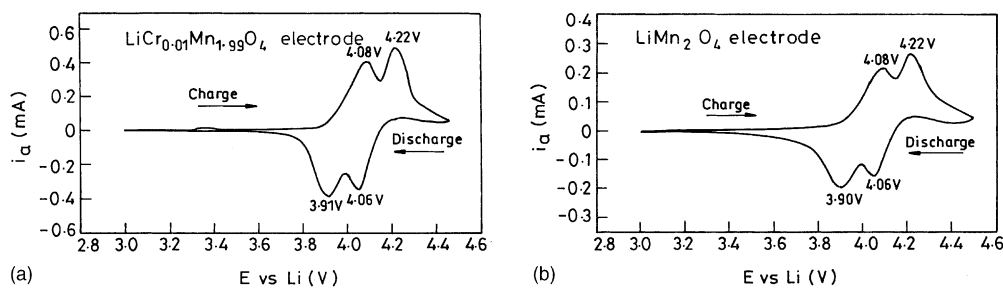


Fig. 6. Cyclic voltammograms for (a) LiMn_2O_4 and (b) $\text{LiCr}_{0.01}\text{Mn}_{1.99}\text{O}_4$ Li at sweep rate 0.02 mV s^{-1} .

fairly tolerant to high voltages [28]. Generally, the anodic and cathodic peaks on the voltammograms are related to the intercalation and de-intercalation of lithium ions into from the spinel. The peak around 4.08 V corresponds to this process at the 8a tetrahedral sites associated with the $\text{Mn}^{4+}/\text{Mn}^{3+}$ couple, while the other peak at 4.22 V corresponds to the oxidation–reduction of Cr^{3+} ions [29,30]. The voltammogram for the chromium-doped spinel reveals that there is an increase in both the anodic and the cathodic peak current. This observation suggests that chromium-doped spinel enhances both reversibility and rate capability.

4. Conclusions

The above study has resulted in the following sentences:

- (i) A new route for the synthesis of LiMn_2O_4 and $\text{LiCr}_x\text{Mn}_{2-x}\text{O}_4$ has been demonstrated via an adipic acid assisted, sol–gel method. This method offers several advantages, i.e., a pure spinel phase, lower calcination temperature, shorter processing time, sub-micron sized particles with a narrow particle-size distribution.
- (ii) XRD and SEM studies confirm high phase purity and well-defined particles with improved morphology, respectively.
- (iii) Charge–discharge studies have established the possibility of enhancing the structural stability of $\text{LiCr}_x\text{Mn}_{2-x}\text{O}_4$ spinels through Cr doping.
- (iv) Cyclic voltammetric experiments disclose the enhanced reversibility and rate capability of Cr^{3+} -modified spinel as compared with undoped spinel.
- (v) The synthesis of $\text{LiCr}_x\text{Mn}_{2-x}\text{O}_4$ ($x = 0.00, 0.01, 0.02, 0.05, 0.10, 0.20$) has resulted in a structurally stabilized spinel with enhanced electrochemical properties.

Acknowledgements

Dr. R. Thirunakaran is grateful to Professor Jai Young-Lee for having arranged a Post Doctoral Fellowship through Brain Korea 21 in order to conduct this research at the Korea Advanced Institute of Science and Technology (KAIST).

References

- [1] Y. Xia, M. Yoshio, J. Electrochem. Soc. 144 (1977) 2593.
- [2] G. Pistoia, A. Antonini, R. Rosati, D. Zane, Electrochim. Acta 41 (1996) 2863.
- [3] D.H. Jang, J.Y. Shin, S.M. Oh, J. Electrochem. Soc. 143 (1996) 2204.
- [4] R.J. Gummow, A. Dckock, M.M. Thackeray, Solid State Ionics 69 (1994) 59.
- [5] A. Yamada, J. Solid State Chem. 122 (1996) 100.
- [6] S.T. Myung, H.T. Chung, S. Komaba, N. Kumagai, H.B. Gu, J. Power Sources 90 (2000) 103.
- [7] T. Ohzuku, S. Takeda, M. Iwanaga, J. Power Sources 81–82 (1999) 90.
- [8] J.H. Lee, J.K. Hong, D.H. Jang, Y.K. Sun, S.M. Oh, J. Power Sources 89 (2000) 7.
- [9] S. Bach, M. Henry, N. Baffier, J.J. Livage, Solid State Chem. 80 (1990) 325.
- [10] J.P. Pereira-Romas, J. Power Sources 54 (1995) 120.
- [11] P. Barboux, J.M. Tarascon, F.K. Shokoohi, J. Solid State Chem. 94 (1991) 185.
- [12] W. Liu, G.C. Farrington, F. Chaput, B.J. Dunn, J. Electrochem. Soc. 143 (1993) 879.
- [13] M.S. Whittingam, Solid State Ionics 86 (1996) 88.
- [14] G. Pistoia, G. Wang, C. Wang, Solid State Ionics 58 (1992) 285.
- [15] W. Baochen, X. Yongyao, F. Li, Z. Dongjinang, J. Power Sources 43–44 (1993) 539.
- [16] L. Guohua, H. Ikuta, T. Uchida, M. Wakihara, J. Electrochem. Soc. 143 (1996).
- [17] A. Mosbach, A. Verbaere, M. Tournoux, Mater. Res. Bull. 18 (1983) 1375.
- [18] M.M. Thackeray, W.I.F. David, P.G. Bruce, J.B. Goodenough, Mater. Res. Bull. 81 (1983) 461.
- [19] W.I.F. David, M.M. Thackeray, P.G. Bruce, J.B. Goodenough, Mater. Res. Bull. 19 (1984) 99.
- [20] W. Borchardt-Ott, Crystallography, Springer, New York, USA, 1993.
- [21] C. Sigala, D. Guyomard, A. Verbaere, Y. Piffard, M. Tournoux, Solid State Ionics 81 (1995) 167.
- [22] D. Zhang, B.N. Popov, R.E. White, J. Power Sources 76 (1998).
- [23] E. Iwata, K. Takahashi, T. Maeda, T. Mouri, J. Power Sources 81–82 (1999) 430.
- [24] C. Sigala, D. Guyomard, A. Verbaere, Y. Piffard, M. Tournoux, Solid State Ionics 81 (1995) 167.
- [25] C. Sigala, M. Tournoux, J. Solid State Chem. 132 (1997) 372.
- [26] H. Kawai, M. Nagata, H. Tukamoto, A.R. West, J. Power Sources 81–82 (1999) 67.
- [27] X. Yia, M. Yoshio, J. Electrochem. Soc. 143 (1996) 825.
- [28] C. Sigala, A. Le Gal La Salle, Y. Piffard, D. Guyomard, J. Electrochem. Soc. 148 (2001) A812.
- [29] C. Sigala, D. Guyomard, A. Verbaere, Y. Piffard, M. Tournoux, Solid State Ionics 81 (1995) 167.
- [30] H. Kawai, M. Nagata, H. Tukamoto, A.R. West, J. Power Sources 81–82 (1999) 67.